

Original Article

Metabolomic profiling and antimicrobial investigation of *Aspergillus fumigatus* LBKURCC269 and *Bacillus paramycoides* LBKURCC218 co-culture

Zona Octarya^{1,2}, Titania T. Nugroho³, Yuana Nurulita³, Nabella Suraya¹ and Saryono Saryono^{3*}

¹Doctoral Program in Chemistry, Faculty of Mathematics and Natural Science, Universitas Riau, Riau, Indonesia; ²Department of Chemistry Education, Faculty of Tarbiyah and Teacher Training, Universitas Islam Negeri Sultan Syarif Kasim Riau, Riau, Indonesia; ³Department of Chemistry, Faculty of Mathematics and Natural Science, Universitas Riau, Riau, Indonesia.

*Corresponding author: saryono@lecturer.unri.ac.id

Abstract

The increasing resistance of pathogenic microbes to antibiotics is a major public health concern, necessitating the discovery of effective antimicrobial compounds. The aim of this study was to assess the bioactive metabolites produced by *Aspergillus fumigatus* LBKURCC269 and *Bacillus paramycoides* LBKURCC218 under three fermentation conditions: monoculture of each microorganism and their co-culture. Metabolite analyses initiated with gas chromatography-mass spectrometry (GC-MS) and liquid chromatography-high-resolution mass spectrometry (LC-HRMS) followed with molecular networking-Global Natural Products Social Molecular Networking (GNPS) and molecular docking. Antimicrobial activity of the extracts was then conducted. Metabolite analysis using GC-MS identified key antimicrobial compounds, including 2,6-bis(1,1-dimethylethyl)-4-methylphenol, pentadecanoic acid, cyclopropane pentanoic acid, and 3-piperidinol. LC-HRMS, combined with multivariate analysis and GNPS molecular networking, revealed additional antimicrobial compounds, including novel pyrazine derivatives induced in co-culture fermentation. Molecular docking analysis of 3-(propan-2-yl)-octahydropyrrolo[1,2-a]pyrazine-1,4-dione demonstrated its potential as an antimicrobial agent by inhibiting topoisomerase IV and cytochrome monooxygenase with binding affinity of -5.34 kcal/mol and -5.6 kcal/mol, respectively. The antimicrobial assays showed that the co-culture fermentation extract had the strongest activity, with inhibition zones of 20.33±0.59 mm (*Escherichia coli*), 14.33±0.59 mm (*Staphylococcus aureus*), and 25.67±0.59 mm (*Candida albicans*). This study highlights the advantages of co-culture fermentation in enhancing the discovery of antimicrobial compounds. The findings underscore the potential of this approach to simplify chemical isolation and accelerate the identification of novel antimicrobial agents for pharmaceutical development.

Keywords: *A. fumigatus*, antimicrobial, *B. paramycoides*, co-culture fermentation, metabolomic profiling

Introduction

The continuous emergence of antimicrobial resistance in pathogenic microorganisms necessitates the discovery of new antimicrobial agents. *Escherichia coli* is one of the most dominant enteric pathogens, responsible for tens of millions of diarrhea cases annually due to its



ability to carry and transfer resistance genes [1]. In addition, high levels of multidrug resistance have been reported in *Staphylococcus aureus* and *Candida albicans*, which together account for more than 50% of eye infections worldwide [2]. The resistance of *S. aureus* isolates in the United States to methicillin has reached 35%, while fluoroquinolone resistance is observed in 32% of isolates [2]. Similarly, in Indonesia, *Staphylococcus* spp. and *E. coli* have been identified as the most common wound-resistant bacterial strains [3]. Given the increasing resistance to existing antimicrobial treatments, researchers have been exploring natural compounds derived from microorganisms in unique and largely unexplored ecosystems as alternative sources for drug discovery.

Thermophilic microbes, which thrive in extreme environments such as hot springs, have emerged as promising candidates for antimicrobial discovery due to their ability to produce bioactive compounds with exceptional stability and activity at elevated temperatures. Previously, we successfully isolated two thermophilic strains-*Aspergillus fumigatus* LBKURCC269 [4] and *Bacillus paramycooides* LBKURCC218 [5] from hot springs in West Sumatra and Riau, Indonesia. These thermophilic microbes have demonstrated the ability to synthesize bioactive compounds with antimicrobial properties. Their adaptation to extreme environments suggests that they may produce unique secondary metabolites with novel mechanisms of action that differ from those of mesophilic microbes [6]. While limited studies have explored the antimicrobial potential of co-cultures involving thermophilic strains, previous studies have successfully isolated antimicrobial compounds from thermophilic microorganisms [7,8]. These findings support the hypothesis that thermophilic microbes, particularly in co-culture systems, could serve as valuable sources for the discovery of new antimicrobial agents.

Co-culture fermentation is a promising strategy for enhancing antimicrobial activity by leveraging microbial interactions to stimulate the production of bioactive compounds [9]. Unlike single-culture fermentation, co-cultures mimic natural microbial ecosystems, where microorganisms engage in dynamic interactions that trigger the activation of silent biosynthetic pathways [10]. These pathways, which often remain dormant in pure cultures, can lead to the synthesis of novel secondary metabolites, including antimicrobial compounds [11]. The key mechanisms driving enhanced metabolite production in co-cultures include microbial competition, environmental stress responses, and quorum sensing, all of which regulate gene expression and activate biosynthetic pathways involved in bioactive compound synthesis [12,13]. Additionally, co-culture fermentation fosters symbiotic metabolism, where one microorganism's metabolites act as precursors or modulators for another, enabling the production of complex antimicrobial agents [14]. By replicating these natural microbial interactions, co-culture fermentation offers a powerful platform for discovering novel bioactive molecules that could address antimicrobial resistance.

Several studies have demonstrated the effectiveness of co-culture fermentation in inducing the production of antimicrobial compounds that are not typically observed in single cultures. For example, the co-culture of *A. fumigatus* with *Streptomyces rapamycinicus* was found to induce the production of the antibacterial compound fumicycline [15]. Similarly, the co-culture of *A. fumigatus* MR2012 with two strains of *S. leeuwenhoekii* (C34 and C58) led to the synthesis of different active compounds [16]. While *A. fumigatus* MR2012 alone produced brevianamide, its co-culture with *S. leeuwenhoekii* C34 resulted in luteoride production, while co-culture with *S. leeuwenhoekii* C58 produced chaxapeptin [16]. These findings highlight the significant influence of microbial interactions on secondary metabolite biosynthesis. Furthermore, the co-culture of *B. amyloliquefaciens* with *Trichoderma asperellum* has been shown to produce antimicrobial compounds with enhanced activity compared to single culture, further emphasizing the potential of microbial co-cultures in the discovery of novel bioactive substances [17].

Recent advancements in metabolomics have facilitated the discovery of antimicrobial compounds in co-culture fermentation by enabling comprehensive analyses of metabolite production. Mass spectrometry (MS)-based metabolomics has been widely used to compare metabolite profiles between single- and co-culture fermentation samples, revealing key differences in compound production. For instance, bioinformatics and metabolomics approaches based on MS data have successfully identified new xylosides in the co-culture of the basidiomycetes *Trametes versicolor* and *Ganoderma applanatum* [18]. Similarly, a previous

study on the endophytic bacterium *S. lunalinharesii* in the presence of the fungal elicitor *R. solani* revealed the production of antifungal compounds desferrioxamine E and anisomycin, as determined through metabolomic analysis [19]. Another study utilized LC-MS/MS analysis to investigate the metabolomic profiles and transcriptomic changes in *Penicillium expansum* 40815 under two distinct fermentation conditions: solid-state fermentation and submerged fermentation [20]. Their findings, presented as molecular networks, identified nine compound clusters induced in co-culture fermentation, many of which exhibited antimicrobial properties [20]. These studies underscore the importance of metabolomics in elucidating microbial interactions and identifying novel antimicrobial compounds. In addition, recent advancements in metabolomics, including multivariate statistical analyses such as principal component analysis (PCA) and partial least squares-discriminant analysis (PLS-DA), as well as molecular network analysis using platforms like MetaboAnalyst and Global Natural Products Social Molecular Networking (GNPS), have significantly improved the efficiency of compound profiling. These techniques enable a detailed comparison of metabolomes between single and co-culture fermentation systems, facilitating the identification of promising antimicrobial compounds.

The aim of this study was to evaluate the antimicrobial activity of the extracts from three fermentation conditions (single cultures of *A. fumigatus* LBKURCC269 and *B. paramycoides* LBKURCC218, as well as their co-culture) and employed GC-MS and LC-MS/MS analyses to identify bioactive metabolites. Additionally, metabolomic analysis was conducted to identify potential new antimicrobial compounds, and molecular docking analysis was performed to predict the interactions between identified bioactive compounds and microbial target proteins, providing insights into their potential mechanisms of action. The selection of *A. fumigatus* LBKURCC269 and *B. paramycoides* LBKURCC218 for co-culture fermentation was based on a previous study demonstrating their high antimicrobial activity [21]. To the best of our knowledge, this is the first study to analyze the metabolite profile of an *A. fumigatus* and *B. paramycoides* co-culture using a combined metabolomic and molecular docking approach for the discovery of novel antimicrobial compounds.

Methods

Microorganism

A. fumigatus LBKURCC269 (accession number OM802493.1) was isolated from the hot spring of Sungai Pinang, Riau, Indonesia, and *B. paramycoides* LBKURCC218 (accession number OM802613.1) was obtained from the hot spring of Rimbo Panti, West Sumatra, Indonesia, are thermophilic microorganisms that have been identified in previous studies [4,5]. The pathogenic microorganisms used, *C. albicans* ATCC 10231, *E. coli* ATCC 35218, and *S. aureus* ATCC 2921, were obtained from the Biochemistry Laboratory of Universitas Riau, Riau, Indonesia.

Aspergillus fumigatus fermentation

The fungal inoculum was collected from a 5-day-old culture stock by cutting a 1×1 cm agar containing fungal mycelia, which was then added to 100 mL of malt extract broth medium as the starter culture. This mixture was incubated for five days at 45°C with shaking at 150 rpm. A 10 mL portion of the inoculum was then transferred to a 1 L Erlenmeyer flask containing 500 mL of malt extract medium and incubated for eight days under the same conditions. At the end of the incubation period, the sample was transferred to a 15 mL conical tube and centrifuged at 3,000 rpm for 30 minutes to obtain a cell-free supernatant [22].

Bacillus paramycoides fermentation

The bacterial strain was grown on nutrient agar (NA) at 45°C overnight. A single colony was then inoculated into 100 mL of malt extract medium and incubated at 45°C with shaking at 150 rpm for 48 hours. The primary sub-cultures were adjusted to an OD₆₀₀ of 0.3, and 10 mL of the diluted culture was further sub-cultured in 500 mL of fresh malt extract medium under the same incubation conditions for another 48 hours. The secondary sub-cultures were then centrifuged at 3,000 rpm for 30 minutes, and the supernatant was collected.

Co-cultured fermentation

A total of 10 mL of *A. fumigatus* LBKURCC269 inoculum was inoculated into 500 mL of malt extract. The mixture was then incubated for three days in an incubator shaker set at 45°C with a speed of 150 rpm. Subsequently, 10 mL of *B. paramycoides* LBKURCC218 inoculum (OD600 of 0.3) was added to 500 mL of *A. fumigatus* LBKURCC269 culture. The incubation process was continued for a further five days [23]. Upon completion of the incubation period, the culture fermentation was subjected to centrifugation for 30 minutes at 3,000 rpm and the supernatant was collected.

Extraction procedure

Ethyl acetate, an organic solvent, was added to the co-culture crude extract and each single culture in a 1:1 ratio using a separating funnel. The resulting crude extract was collected and concentrated with a rotary evaporator at 50°C, then further dried in a water bath at 45°C with gentle rotation at 100 rpm. The dried extracts were then subjected to antimicrobial activity tests [24]. Changes in the secondary metabolite profiles between co-culture and single-culture fermentation were analyzed using gas chromatography-mass spectrometry (GC-MS) and liquid chromatography-high-resolution mass spectrometry (LC-HRMS).

Gas chromatography-mass spectrometry (GC-MS) analysis

A 3 µL sample was injected at 300°C, with a gas chromatography (GCMS-QP2010, Shimadzu corporation, Kyoto, Japan) run time of 80 minutes. The column used was a silica fusion Rtx (Restek Corporation, Bellefonte, PA USA) with a length of 30 m, a diameter of 250 µm, and a thickness of 0.25 µm. The electron energy applied was 70 electron volt (eV), and the detected mass range was 28–600 atomic mass unit (amu). Helium gas was used as the carrier, with a flow rate of 0.5 mL/min and a pressure of 13.7 kilopascal (kPa). The resulting chromatograms were compared with compounds in the database [25]. Subsequently, the molecular formula, chemical structure, and name of the compound produced under each fermentation condition were identified.

Liquid chromatography-high-resolution mass spectrometry (LC-HRMS) analysis

The dried extract was ultrasonically extracted using methanol (Branson Ultrasonic Corporation, Danbury, CT, USA). The LC-HRMS analysis was performed on a Vanquish Flex UHPLC-Q Exactive Plus Orbitrap system equipped with an Accucore C18 column (100×2.1 mm, 1.5 µm) and a UV detector set at 254 nm (Thermo Fisher Scientific, Bremen, Germany). Electrospray ionization (ESI) was used as the MS ionization source, and a Q-Orbitrap served as the mass analyzer. The flow rate of the delivery system was set at 0.2 mL/min, with a sample injection volume of 5 µL. The mobile phases used were 0.1% formate in water/acetonitrile (A) and 0.1% formate in water/acetonitrile (B). Fragmentation collision energies were set at 18, 35, and 53 eV. Other analytical conditions included a spray voltage of 3.8 kV, a capillary temperature of approximately 320°C, and shielding gas and carrier gas flow rates of 15 and 3 mL/min, respectively. A linear gradient elution program was applied with the following time points: 0–1 min (5% B), 1–25 min (5–95% B), 25–28 min (95% B), and 28–30 min (5% B). The MS analysis was conducted in positive mode using a full scan range of 100–1500 m/z, with a relative abundance range of 0–100, for a total run time of 30 min.

Molecular networking–Global Natural Products Social Molecular Networking (GNPS)

The LC-HRMS data was converted from .d to .mzXML format using MSConvert software. The cross-platform FTP client FileZilla was used to upload the converted mzXML files to the GNPS server (massive.ucsd.edu). Precursor and fragment ion mass tolerances were set to 0.02 Da for molecular network construction. The following parameters were applied: minimum pair cosine of 10, maximum mesh size of 100, maximum number of matched fragments of 4, and a minimum cluster size of 2. For the library search, the minimum number of peaks required for a match was set to 4, with a score threshold of 0.65. Default values were used for all other parameters. The data was then preprocessed to remove noise and identify relevant mass features. The GNPS

carried out the feature detection and mass matching to identify similarities with known compounds. The platform uses similarity-based algorithms to construct a molecular network by linking mass features with similar fragmentation patterns, reflecting structural or biosynthetic relationships between compounds. The constructed molecular network was visualized interactively, allowing for the identification of clusters of related compounds. The next step involved compound identification by comparing fragmentation patterns with reference databases: MassBank (<https://massbank.eu>) or Human Metabolome Database (HMDB) (<https://hmdb.ca>). After network analysis, statistical methods like clustering were applied to identify families of compounds with similar structures [26]. Cytoscape version 3.6.0 (Cytoscape Consortium, San Diego, United States) was used to construct the molecular network [27].

Molecular docking analysis of potential metabolites

The docking analysis was performed using MOE 2020.0102 software, (<https://www.chemcomp.com/en/Products.htm>). During protein preparation, the 3D structure of DNA topoisomerase IV and cytochrome monooxygenase was retrieved from the Protein Data Bank (PDB) (<https://www.rcsb.org>) with the accession number 4EMV and 5V5Z, respectively. MOE was used to remove crystal water, add Gasteiger charges to each atom, and merge the non-polar hydrogen atoms into the protein structure. During ligand preparation, Chem3D Ultra 19 (ChemOffice, PerkinElmer, Waltham, USA) was used to draw the structures of ligands oR9 (5-(2-(ethylcarbamoyl)-4-(3-(trifluoromethyl)-1H-pyrazol-1-yl)-1H-pyrrolo(2,3-b)pyridin-5-yl)pyridine-3-carboxylic acid), 1YN (2-((2R)-butan-2-yl)-4-(4-(4-(4-(((2R,4S)-2-(2,4-dichlorophenyl)-2-(1H-1,2,4-triazol-1-yl)methyl)-1,3-dioxolan-4-yl)methoxy)phenyl)piperazin-1-yl]phenyl)-2,4-dihydro-3H-1,2,4-triazol-3-one), HEM (protoporphyrin IX containing Fe) and potential metabolites. The preparation of ligands and the protein model, as well as the docking process, were conducted using MOE 2020.0102 software. The energy was minimized to a minimum root mean square (RMS) gradient of 0.0001 in each iteration with the Merck Molecular Force Field 94 (MMFF94) force field model, and subsequently utilized for docking studies. Both the protein and ligand structures were then saved in PDBQT file format for docking in MOE. The docking protocol followed the method outlined previously [28]. Finally, the docking results were visualized in 2D and 3D using BIOVIA Discovery Studio Visualizer 2019 software (BIOVIA Discovery Studio Visualizer 2019 software, San Diego, United States) (<https://discover.3ds.com/discovery-studio-visualizer-download>).

Antimicrobial activity of fermentation extracts

The antimicrobial activity of ethyl acetate extracts obtained from the three fermentation conditions was evaluated against three microbial pathogens, *C. albicans*, *E. coli*, and *S. aureus*, using the agar diffusion method. A 20 μ L aliquot of the extract (120 ppm) was dispensed onto sterilized disc paper and placed on agar media (Merck, KGaA, Germany) previously inoculated with a suspension of the target microbes. Disc paper containing 5 μ L of ampicillin (120 μ g/mL) served as the positive control for bacterial strains, while nystatin was used as the positive control for fungal strains. The plates were incubated at 37°C for 24 hours.

Data analysis

MS-DIAL version 6.0 (Riken Center for Sustainable Resource Science, Yokohama, Japan) was used for the qualitative analysis of compounds, including peak discrimination, filtering, and alignment. Abf Converter 4.0.0 (.abf format) and MS FileReader 2.2.62 were used to import raw MS data (raw format). A mass error value of 10 ppm was applied as a filtering criterion for scanning experiments. Fragmentation patterns (MS and MS/MS) were analyzed using Compound Discoverer software (Thermo Scientific, Waltham, USA) and freely available fragmentation algorithms such as MS-FINDER.

A hierarchical cluster analysis heatmap was generated to visualize the putatively identified compounds in monoculture and co-culture fermentation extracts. MetaboAnalyst 6.0 (<https://www.metaboanalyst.ca>) was used to construct the heatmap based on peak area data (*.csv format) for all detected compounds in the adduct type (M+H⁺) of each fermentation condition.

PCA and PLS-DA analysis using MetaboAnalyst 6.0 (<https://www.metaboanalyst.ca>) were performed to analyze data obtained from LC-HRMS. Tukey's honest significant difference (Tukey's HSD) test was used for multiple pairwise comparisons between groups. Differences in metabolite profiles between sample classes were visualized using PCA, while PLS-DA was used to identify metabolites based on the following cutoffs: variable importance in prediction (VIP) >1 and adjusted false discovery rate (FDR) <0.05. Cross-validation and permutation tests were conducted to ensure that the PLS-DA model did not classify samples by chance. The quality of the PLS-DA model was assessed using $R^2(Y)$ and $Q^2(Y)$ statistics. $R^2(Y)$ represents the goodness of fit, indicating the proportion of variance in Y that is explained by the model, while $Q^2(Y)$ reflects the model's predictive ability [17].

Antimicrobial results are expressed as the mean \pm SD of three replicates for each sample. One-way ANOVA was performed using Minitab version 19.0 (Minitab, State College, USA), and Duncan's multiple range test was used for mean comparisons when ANOVA indicated significant variation at a significance level of $p=0.05$.

Results

GC-MS analysis and secondary metabolite profiling using LC-HRMS analysis

The volatile compounds produced in the co-culture fermentation from highest to lowest composition are presented in (Table 1). The most dominant compound increased in the co-culture fermentation was the 2,6-bis(1,1-dimethylethyl)-4-methyl phenol. The metabolites 2,6-bis(1,1-dimethylethyl)-4-methyl phenol, tetradecane, 2-(1,1-dimethylethyl)sulfonyl-2-methyl propane, pentadecane, and octadecane were found to be produced in higher amounts during co-culture fermentation compared to single culture fermentation. This increase was quantified based on the peak area of each compound as detected in the GC-MS chromatogram. In single culture fermentation, the percentage peak areas of these compounds were 4.15%, 0.81%, 0.87%, 0.70%, and 1.76%, respectively. During co-culture fermentation, these percentages increased significantly to 10.39%, 2.54%, 7.72%, 4.91%, and 6.52%, respectively. These results indicate that co-culture fermentation enhanced the production of certain metabolites, likely due to interactions between microorganisms that trigger the production of additional or unique compounds.

Based on the ions extracted from the mass spectrum, 7,274 molecular entities were detected using MS-DIAL software. Peak intensity analysis using MetaboAnalyst software generated a heat map, revealing differences between the monoculture and co-culture extracts, as well as between the co-culture extract and the blank. Interestingly, certain metabolites were exclusively induced in co-culture fermentation (Figure 1). Metabolites produced at high levels are shown in red, while those produced at low levels are shown in blue (Figure 1). The PCA plot showed that the two main principal components (PCs) accounted for 92.4% of the total variability. PC-1 contributed 61.6%, while PC-2 accounted for 30.6% (Figures 2A1 and 2A2). With cumulative percentage of total variance of 92.4%, this indicated that the PCA used for sample grouping has high accuracy in distinguishing the three fermentation models, as reflected in the substantial variance captured by PC-1 and PC-2 [29].

Table 1. Metabolites identified in the *Aspergillus fumigatus* and *Bacillus paramycoide* co-culture by gas chromatography-mass spectrometry (GC-MS) analysis

Compound	Retention time (min)	Production in co-culture	Similarity index (%)
2,6 bis(1,1 dimethylethyl) 4-methyl phenol	27.504	Increase	78
Pentadecanoic acid	36.696	On	93
Tetradecane	51.379	Increase	93
Carbamic acid	9.146	On	88
2-(1, 1 dimethylethyl) sulfonyl 2 methyl propane	69.761	Increase	81
Cyclopropane pentanoic acid	40.203	On	92
Pentadecane	51.548	Increase	92
Octadecane	56.254	Increase	94
Eicosyltrichlorosilane	37.988	On	93
1,2,4-trimethyl benzene	9.226	On	90
1-dodecene	41.836	On	88
2-octanone	37.692	On	78

Compound	Retention time (min)	Production in co-culture	Similarity index (%)
Silane	33,746	On	92
1,1 cyclopropane dicarbonitrile	9,358	On	67
2-buthyl 1-octanol	54,462	On	91
2-methyl dodecane	38,098	On	94
1,2,3 trimethyl benzene	7,800	On	87
2,7 dimethyl undecane	37,444	On	90
2,2-dimethyl 4-decane	63,115	On	77
3-piperidinol	21,099	On	55
4-methyl tridecane	37,292	On	76
Nonane	33,251	On	86
2-ethyl 1-decanol	57,644	On	87
3,3-dimethyl hexane	20,249	On	92
Ethyl linolenate	44,242	On	58

Increase: increased metabolite production in co-cultured compared to a single culture; On: ex novo co-cultured metabolite

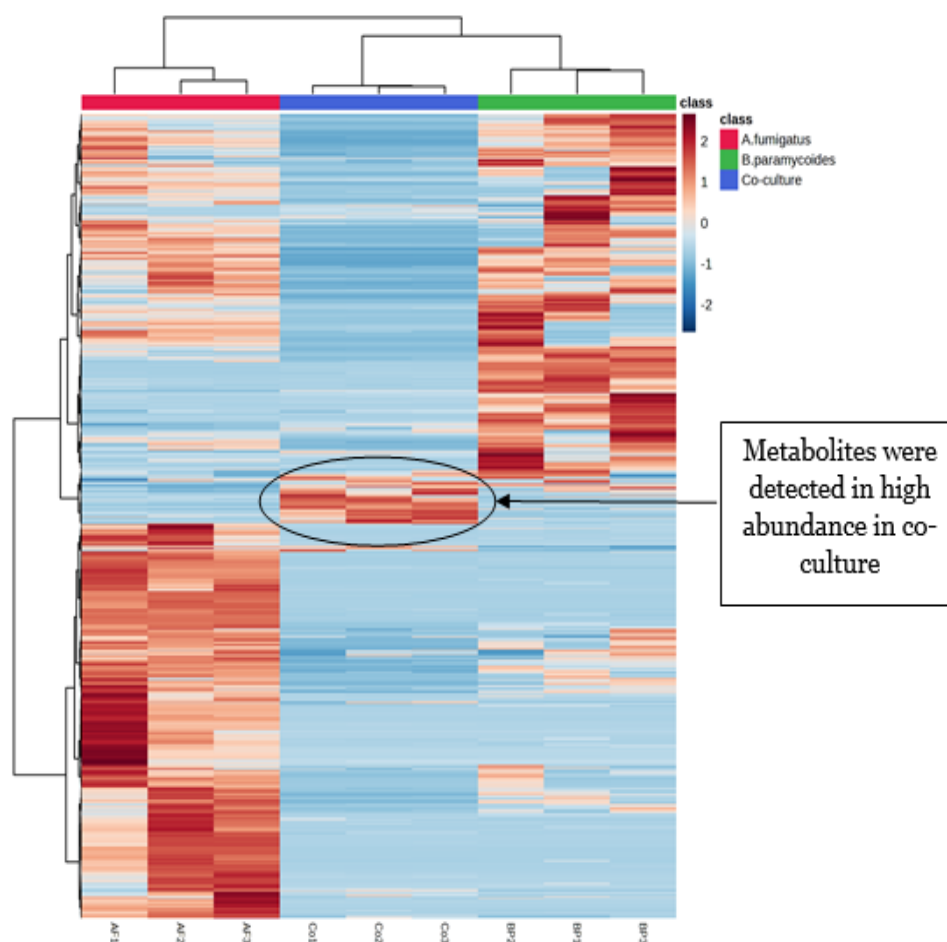


Figure 1. Comparison of metabolite profiles across three fermentation conditions. Multivariate data analysis using MetaboAnalyst software, hierarchical clustering, and heatmap correlation. Each colored cell in the heatmap represents the average peak intensity value. Columns represent fermentation treatments and rows represent metabolites produced. Red indicates an increase and blue indicates a decrease.

PLS-DA of the Orbitrap UHPLCQ-HRMS data peaks also revealed intrinsic variation in the data set. In the score plot, samples from the co-culture were separated from the single cultures, indicating a change in metabolite profiles (**Figures 2B1** and **2B2**). Based on PCA and PLS-DA analysis, marker compounds that discriminated between extracts from each single fermentation and the co-culture are presented in (**Table 2**). Five marker compounds were identified based on the LC-MS/MS database: zalcitabine, linoleamide, (Hydroxyethyl)methacrylate, 4-aminophenol-1, and methylbutylnitrosamine. The other four (metabolites 2, 3, 5, 6) are likely to be novel compounds.

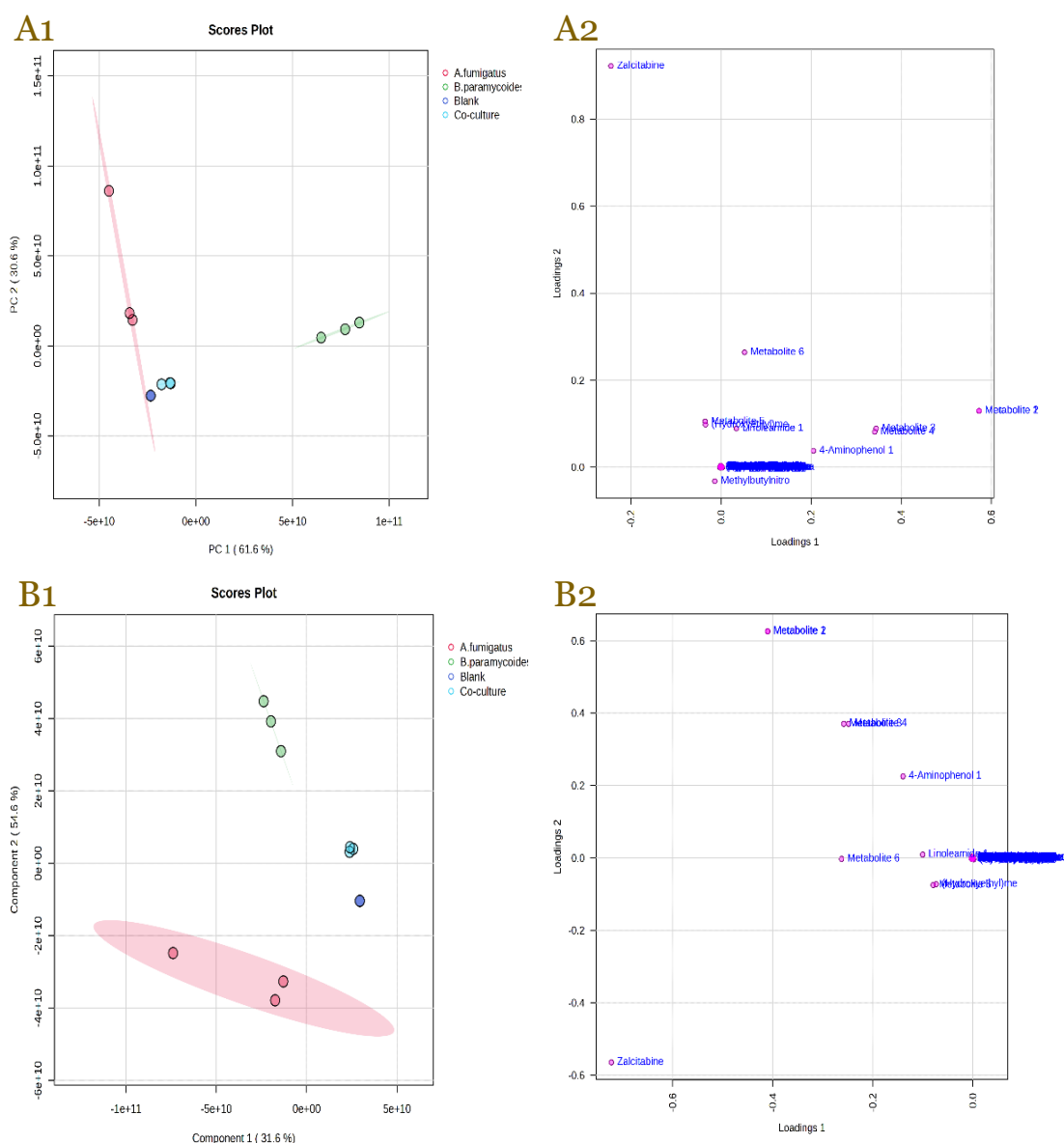


Figure 2. Principal component analysis (PCA) and partial least squares discriminant analysis (PLS-DA) analyses of metabolite profiles from three fermentation conditions. Multivariate data analysis using MetaboAnalyst software. (A1) PCA biplot for principal components; (A2) PCA loading plot for principal components (PC-1) and (PC-2); (B1) PLS-DA biplot for principal components (Component-1) and (Component-2); (B2) PLS-DA loading plot for main components (Component-1) and (Component-2) at three fermentation conditions using UHPLC-Q-Orbitrap HRMS data.

Table 2. Marker compounds to differentiate between single cultures of *Aspergillus fumigatus* and *Bacillus paramycoide* and co-culture of both

Compounds name	m/z
Zalcitabine	211.14326
(Hydroxyethyl)methacrylate	130.1430
Methylbutylnitrosamine	116.10732
Metabolite 5	124.03922
Linoleamide	270.15857
Metabolite 6	197.12819
4-Aminophenol 1	109.5736
Metabolite 2	273.18472
Metabolite 3	227.17531

In PLS-DA, metabolites were assigned a variable importance in projection (VIP) score, where higher values indicate greater significance (**Figure 3**). Our data indicated that the metabolite concentrations were changed across the three fermentation conditions (**Figure 3**). Five compounds were found in high concentrations under co-culture fermentation, including methylbutylnitrisamine (m/z 116.10732), 2-(4-hydroxybenzyl)-4-(3-acetyl)quinazolinone (m/z 295.14145), mefenamic acid (m/z 241.99968), (aminomethyl)phosphonate (m/z 112.00661), and brevianamide (m/z 284.13848) (**Figure 3**). Hierarchical clustering analysis (HCA) of 117 molecular features based on MS data further confirmed that co-culture fermentation alters metabolite production (**Figure 4**).

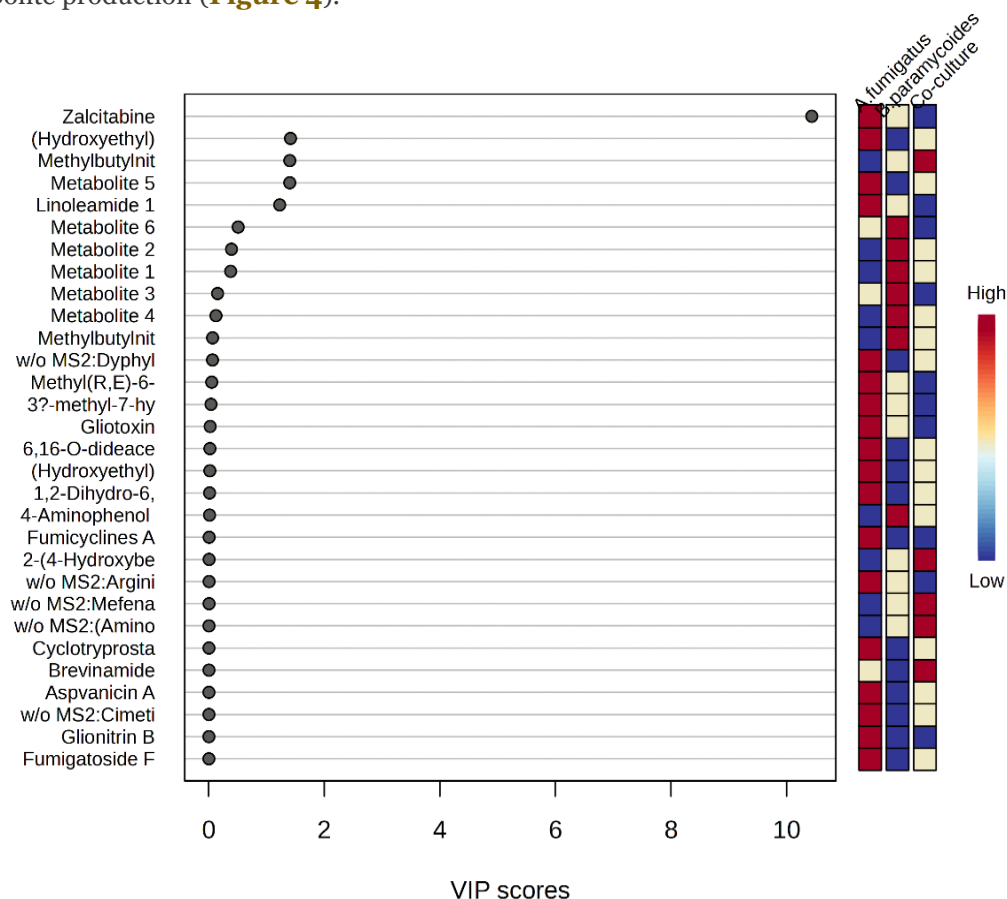


Figure 3. Variables Importance in the Projection (VIP) score plot for 30 metabolites with maximum abundance in monoculture of *Aspergillus fumigatus*, *Bacillus paramycoide* and their co-culture. The colored boxes on the right illustrate changes in metabolite concentrations across the three fermentation conditions.

Molecular analysis of metabolites induced in co-culture with GNPS

The profiles of antimicrobial compounds produced by single culture and co-cultures of *A. fumigatus* and *B. paramycoide* were further analyzed using GNPS. GNPS is linked to organic compound databases such as PubChem, Natural Product Atlas, Dictionary of Natural Products (DNP), Natural Product Activity and Species Source Database (NPASS), Natural Product Atlas, and National Institute of Standards and Technology (NIST). GNPS produces a complex network of nodes grouped into clusters. Each node represents an ion found in at least one growth culture, and different colors are used to define different groups of compounds. The metabolite network of *A. fumigatus* (G1) and *B. paramycoide* (G2) and their co-culture (G3) was generated using the GNPS molecular network, resulting in 2242 nodes and 2834 edges, which were divided into 65 submolecular networks. From the results of the GNPS analysis, 21 compound clusters were obtained and the results are presented in (**Table 3**). Interestingly, the molecular network highlighted four sub-clusters of compounds induced under co-culture conditions, including indoles and derivatives (five ions generated on co-culture), tryptamine (one ion generated on co-culture), myristoyl-3-phosphoethanolamine (four ions generated on co-culture) and pyrazine (three ions generated on co-culture) (**Figure 5**).

Detailed information on the 21 annotated clusters, including their library classification, cosine values, m/z data, ionization method, and instrumentation, is presented in (Table 3). The experimental mass spectra closely matched the library spectra, with compounds such as pyrazino[1,2-a]indole-1,4-dione, 3-indolelactic acid, and (S,S)-asperphenamate achieving "gold level" classification and a cosine value of 0.95, confirming their tentative identification in the ethyl acetate extract. These annotations were validated using the GNPS platform, which highlighted the high quality of spectral matches based on mass accuracy, instrument resolution, and metadata. Additionally, the Bioinformatics and Molecular Design Research Center Mass Spectral Library (BMDMS-NP) confirmed the reliability of the results, as the reference data for these metabolites were generated using the same orbitrap instrument employed in this study.

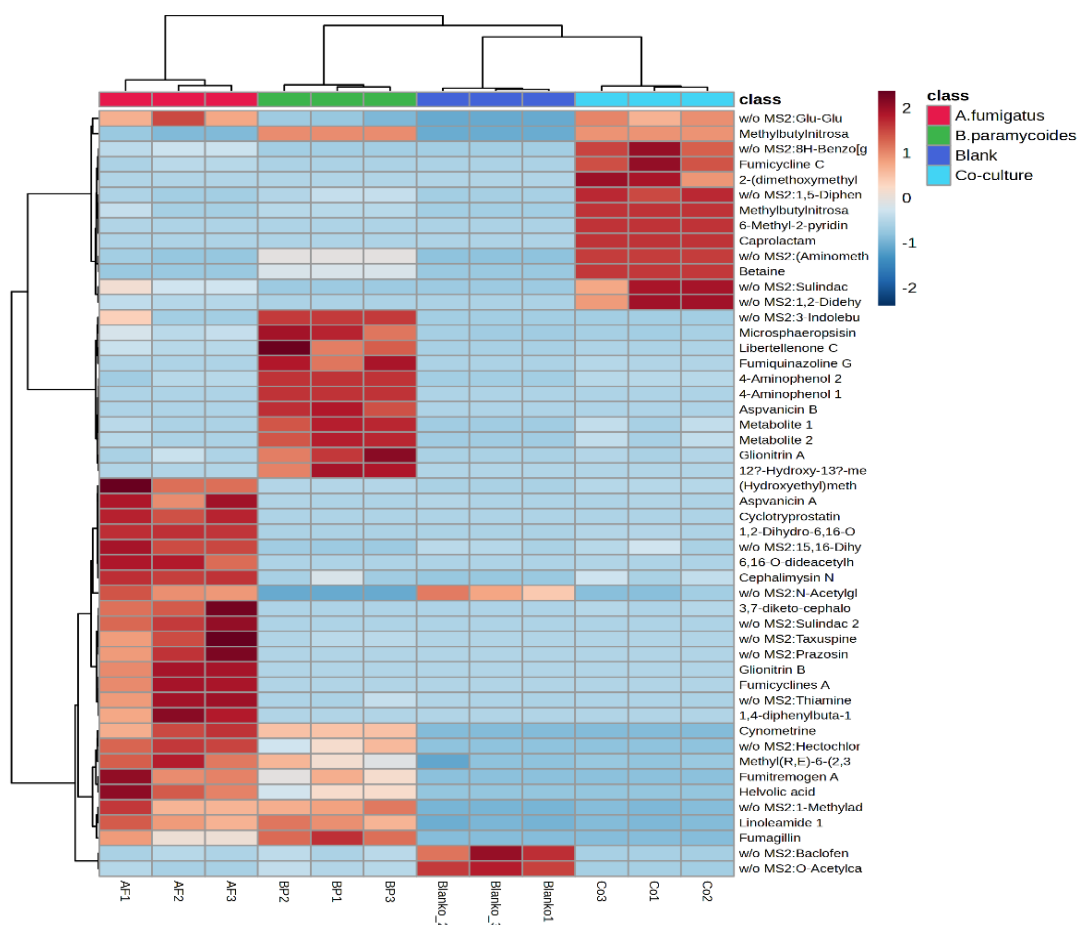


Figure 4. Hierarchical clustering and heatmap correlation of the 117 identified metabolites from monoculture of *Aspergillus fumigatus*, *Bacillus paramycoide* and their co-culture. Each colored cell in the heatmap represents the average peak intensity value. Columns represent fermentation treatments and rows represent metabolites produced. Red indicates an increase and blue indicates a decrease in concentration.

Molecular docking

The antimicrobial metabolites induced during co-culture fermentation, identified as N7 and N8, were analyzed using GNPS molecular networking (Figure 5). The analysis revealed that these compounds have clusters closely related to 3-(propan-2-yl)-octahydropyrrolo(1,2-a)pyrazine-1,4-dione, suggesting structural similarities and potential functional relevance. Given this relationship, N7 and N8 are considered promising candidates as novel antimicrobial agents. The 3-(propan-2-yl)-octahydropyrrolo(1,2-a)pyrazine-1,4-dione was then evaluated as a ligand, with ampicillin and nystatin serving as positive controls for antibacterial and antifungal activity, respectively.

Table 3. Library hits from Feature-Based Molecular Networking in Global Natural Products Social Molecular Networking (GNPS)

Compound clusters	Compound name	Cluster index	Formula	Spectral m/z/Library m/z	MZ error (ppm)	Ion source	Instrument	Library class	Cosine	Data source
Indol derivates	Pyrazino[1,2-a]indole-1,4-dione, 2,3,5a,6,10,10a-hexahydro-6-hydroxy-3-(hydroxymethyl)-2-methyl-3,10a-bis(methylthio)-, (3R,5aS,6S,10aR)	3592	C ₁₂ H ₇ N ₃ O ₂	357.094/357.094	0	LC-ESI	Maxis II HD Q-TOF Bruker	Gold	0.71	Jadhav/Doerrestein
Indol	dl 3-Indolelactic acid	324	C ₉ H ₉ NO ₂	204.07/204.07	2	ESI	Orbitrap	Gold	0.86	Massbank
3-Epilupeol	3-Epilupeol	4660	C ₁₅ H ₂₄ O	427.39/427.39	9	ESI	ESI-QFT	Bronze	0.73	MoNA
3-Phosphoethanolamine	1-Palmitoyl-2-hydroxy-sn-glycero-3-phosphoethanolamine	4871	C ₁₆ H ₃₇ NO ₅ P	452.28/452.28	0	ESI	Qtof	Bronze	0.81	Kevin Bush
	1-Myristoyl-2-hydroxy-sn-glycero-3-phosphoethanolamine	4630	C ₁₄ H ₂₉ NO ₅ P	426.26/426.26	21	ESI	HCD	Bronze	0.86	Pieter dorrestein
	1-Stearoyl-2-hydroxy-sn-glycero-3-phosphoethanolamine	5102	C ₁₈ H ₃₇ NO ₅ P	482.32/482.32	0	ESI	qTof	Bronze	0.79	Wolfender/litaudon
Cinnamic acid	Octyl-methoxycinnamate octinoxate 2-ethylhexyl (E)-3-(4-methoxyphenyl)prop-2-enoate	1930	C ₁₈ H ₂₆ O ₃	291.19/291.19	0	ESI	qTof	Bronze	0.91	Massbank
Asperphenamate	Asperphenamate	5239	C ₁₄ H ₁₅ NO ₂	507.23/507.23	1	LC-ESI	Qtof	Silver	0.92	Cichewicz
	(S,S)-asperphenamate	5356	C ₃₀ H ₃₀ N ₂ O ₆	529.21/529.21	0	ESI	Orbitrap	Gold	0.8	BMDMS-NP
Bis-2-ethylhexyl phthalate	Hexanedioic acid, bis(2-ethylhexyl) ester	3844	C ₂₂ H ₄₂ O ₄	371.31/371.32	2	ESI	Qtof	Bronze	0.97	Piel
	Bis(2-ethylhexyl) phthalate	4174	C ₂₄ H ₃₈ O ₄	391.28/391.28	2	ESI	QQQ	Bronze	0.97	Gabriel haddad
Carboxylic acid	9-(2,3-dihydroxypropoxy)-9-oxononanoic acid	1277	C ₁₂ H ₂₂ O ₆	261.13/261.13	3	ESI	ESI-QFT	Bronze	0.89	MoNA
	Oleic acid	1366	C ₁₈ H ₃₄ O ₂	265.25/265.25	0	LC-ESI	Orbitrap	Bronze	0.84	Trent Northen
Depsipeptide	Cyclo(L-Val-L-Pro)	230	C ₁₀ H ₁₆ N ₂ O ₂	197.13/197.13	5	DI-ESI	qTof	Bronze	0.85	Keyzers
	Cyclo(Phe-4-Hyp)	1271	C ₁₃ H ₁₆ N ₂ O ₃	261.12/261.12	1	DI-ESI	qTof	Bronze	0.86	Keyzers
	Cyclo(leucylprolyl)	403	C ₁₁ H ₁₈ N ₂ O ₂	211.14/211.14	0	ESI	qTof	Bronze	0.9	Massbank
	Cyclo(Phe-Leu)	1278	C ₁₅ H ₂₀ N ₂ O ₂	261.16/261.16	3	DI-ESI	qTof	Bronze	0.74	Keyzers
Dibutyl phthalate	Dibutyl Phthalate	1642	C ₁₆ H ₂₂ O ₄	279.16/279.16	3	ESI	QqQ	Bronze	0.93	Pieter dorrestein
Glycerolipid	Monoolein	3608	C ₁₈ H ₃₄ O ₃	357.3/357.30	0	LC-ESI	Orbitrap	Bronze	0.83	Trent Northen
	1-Hexadecanoyl-sn-glycerol	3058	C ₁₉ H ₃₈ O ₄	331.28/331.29	3	ESI	qTof	Bronze	0.85	Piel
	Glycerol 1-stearate	3647	C ₂₁ H ₄₂ O ₄	359.32/359.32	11	ESI	QQQ	Bronze	0.78	Piel
Alicyclic	1,3,4,6,7,8-Hexahydro-4,6,6,7,8,8-hexamethylcyclopenta(g)-2-benzopyran-1-on	1526	C ₁₈ H ₂₆ O ₂	273.19/273.19	0	ESI	LC-ESI-ITFT	Bronze	0.88	Massbank
Lauryl diethanolamide	Lauryl diethanolamide	1859	C ₁₆ H ₃₃ NO ₂	288.25/288.25	0	LC-ESI	Orbitrap	Gold	0.95	CASMI
Octadecatrienoic acid	9Z,11E,13E-Octadecatrienoic acid methyl ester	1990	C ₁₉ H ₃₂ O ₂	293.25/293.25	0	ESI	HCD	Bronze	0.95	Wolfender/litaudon
Fatty acid esters	Linoleic acid	1689	C ₁₈ H ₃₂ O ₂	281.25/281.25	0	LC-ESI	qTof	Bronze	0.74	MoNA
	Keto-9Z,11E-octadecadienoic acid	1618	C ₁₈ H ₃₀ O ₃	277.22/277.22	0	ESI	HCD	Bronze	0.77	Wolfender/litaudon
	12(13)-Epoxy-9Z-octadecenoic acid	1648	C ₁₈ H ₃₂ O ₃	279.23/279.23	7	ESI	qTof	Bronze	0.77	Wolfender/litaudon

Compound clusters	Compound name	Cluster index	Formula	Spectral m/z/Library m/z	MZ error (ppm)	Ion source	Instrument	Library class	Cosine	Data source
Octadecadienol	cis,cis-9,12-Octadecadien-1-ol	1391	C ₁₈ H ₃₂ O	267.27/267.27	0	ESI	HCD	Bronze	0.86	Wolfender/litaudon
Octadecanamide	Octadecanamide	1751	C ₁₈ H ₃₇ NO	284.3/284.30	17	ESI	QqQ	Bronze	0.78	Wolfender/litaudon
	9-Octadecenamide	1751	C ₁₈ H ₃₅ NO	284.3/284.30	0	ESI	QqQ	Bronze	0.78	Wolfender/litaudon
	13-Docosenamide	3159	C ₂₂ H ₄₃ NO	338.34/338.34	0	ESI	HCD	Bronze	0.79	Wolfender/litaudon
Pyrazine	3-((4-hydroxyphenyl)methyl)-2,3,6,7,8,8a-hexahydropyrrolo(1,2-a)pyrazine-1,4-dione	1270	C ₁₃ H ₁₄ N ₂ O ₃	261.12/261.12	0	LC-ESI	Maxis II HD Q-TOF Bruker	Gold	0.74	Jadhav/dorrestein
Polyethylene glycol	3,6,9,12-Tetraoxatetracosan-1-ol Tetraethylene glycol monododecane	3707	C ₁₈ H ₃₈ O ₆	363.31/363.31	0	ESI	qTof	Bronze	0.88	Massbank
	Tetraoxatetracosane 1-nol	2467	C ₁₀ H ₁₈ O ₃	311.17/311.15	61	ESI	ESI-QFT	Bronze	0.79	MoNA
Tryptamine	Tryptamine-C19:0	4783	C ₁₉ H ₃₈ O ₂	441.38/441.38	2	ESI	qTof	Silver	0.93	Dorrestein
	Tryptamine-C17:0	4477	C ₁₇ H ₃₄ O ₂	413.35/413.35	0	ESI	qTof	Silver	0.96	Dorrestein
	Tryptamine C:16	4296	C ₁₅ H ₃₂ O ₂	399.34/399.34	0	ESI	qTof	Silver	0.95	Dorrestein

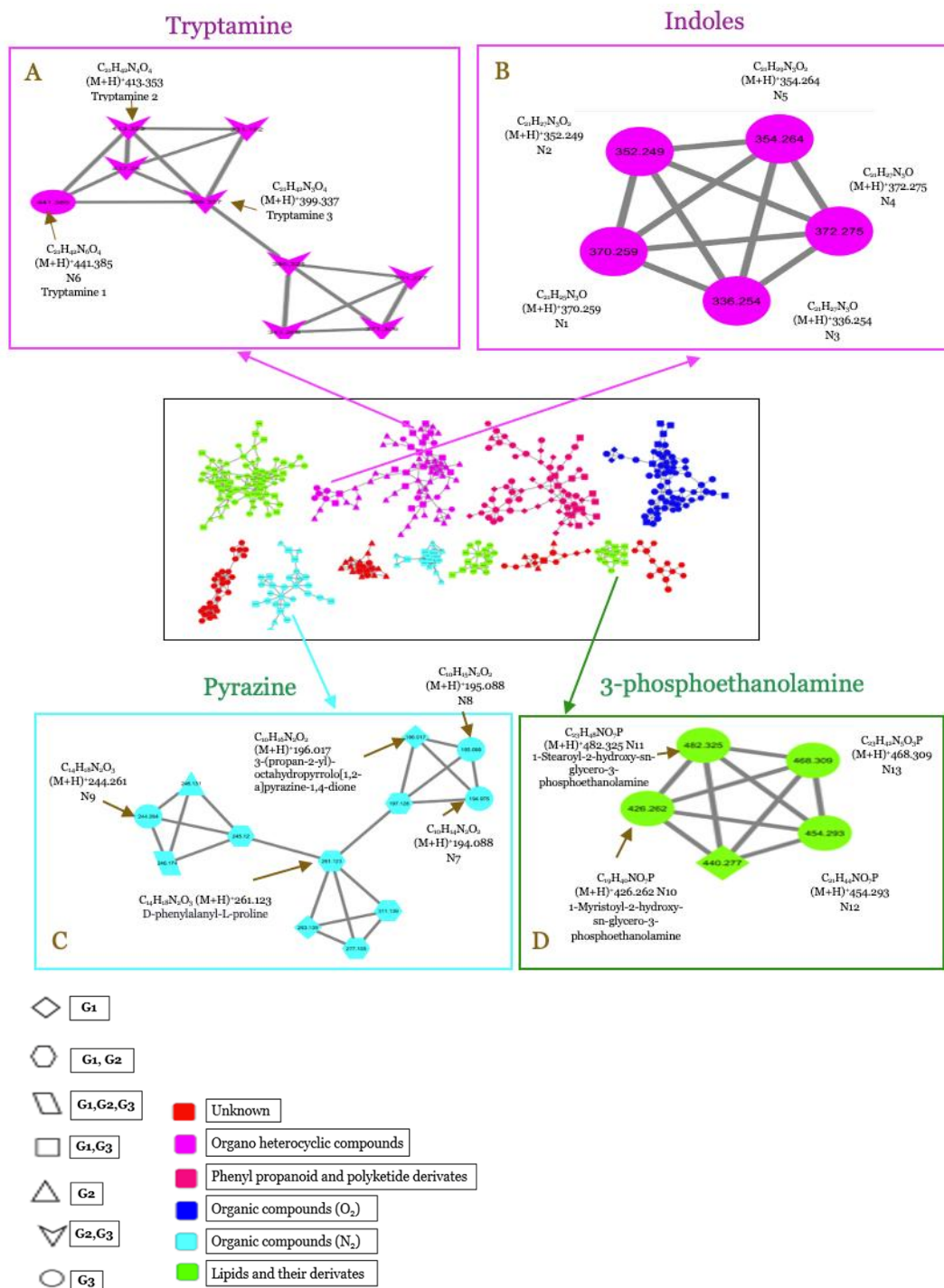


Figure 5. Molecular network analysis of compounds induced in co-culture fermentation by Global Natural Products Social Molecular Networking (GNPS), indoles and derivatives (A), tryptamine (B), pyrazine (C), and myristoyl-3-phosphoethanolamine (D). The shape of the symbols indicates the fermentation conditions, and the different colors represent the grouping of metabolite types, sub-clusters of compounds produced in the fermentation of *A. fumigatus* (G1) and *B. paramycooides* (G2) and their co-cultured (G3) obtained by CytoCluster application in Cytoscape.

Furthermore, their potential to inhibit key enzyme receptors, including topoisomerase IV (4EMV) and cytochrome monooxygenase (5V5Z), were investigated to assess their effectiveness as antibacterial and anticandidal agents. The results of molecular docking of 3-(propan-2-yl)-octahydropyrrolo(1,2-a)pyrazine-1,4-dione against topoisomerase IV and cytochrome monooxygenase CYP51 are presented in (Table 4).

Table 4. Molecular docking results of 3-(propan-2-yl)-octahydropyrrolo(1,2-a)pyrazine-1,4-dione against topoisomerase IV and cytochrome monooxygenase CYP51 enzymes

Compounds	Target enzyme			
	Topoisomerase IV		Cytochrome monooxygenase CYP51	
	Binding affinity (kcal/mol)	Root mean square deviation(RMSD)	Binding affinity (kcal/mol)	Root mean square deviation (RMSD)
3-(Propan-2-yl)-octahydropyrrolo(1,2-a)pyrazine-1,4-dione	-5.34	1.36	-5.6	1.255
Ampicillin	-5.08	0.78		
OR9 (ligand for topoisomerase IV enzyme)	-9.04	2.3		
Nystatin			-11.2	2.0
1YN, HEM (ligand for cytochrome monooxygenase enzyme)			-11.61	2.1

3-(Propan-2-yl)-octahydropyrrolo(1,2-a)pyrazine-1,4-dione showed higher effectiveness to the topoisomerase IV enzyme receptor compared to control but lower than the native ligand with an affinity of -5.34 kcal/mol and lower effectiveness to the cytochrome monooxygenase CYP51 enzyme receptor compared both to the control and the native ligand with an affinity of -5.6 kcal/mol. This visualization aimed to identify the residues involved in hydrogen bonds and hydrophobic interactions between the ligand and the receptors (**Figure 6**).

The molecular docking analysis of topoisomerase IV demonstrated significant interactions between the receptor and the compound, primarily through hydrogen bonds, hydrophobic interactions, and van der Waals forces. Key residues such as GLY82 and THR172 were involved in hydrogen bonding, while PRO84 and MET83 contributed to hydrophobic interactions that stabilized the ligand within the binding pocket of topoisomerase IV (**Figure 6B**). The strong hydrogen bond between the ligand and GLY82 and THR172 were observed within the active site of topoisomerase IV and this region is crucial for its ligand binding and enzymatic inhibition [30]. The presence of good least binding interactions suggested that the compound has the potential to interfere with the function of topoisomerase IV, which is essential for bacterial DNA replication, thereby supporting its possible antibacterial activity. Similarly, the docking results for cytochrome monooxygenase revealed that the compound interacted within the enzyme's active site through a combination of hydrogen bonds and hydrophobic interactions. Residues such as SER378 played a key role in hydrogen bond, while MET508 was involved in hydrophobic stabilization (**Figure 6C**). The good interaction within this region suggests that the compound may influence the enzymatic activity of cytochrome monooxygenase, potentially affecting its role in metabolic processes.

Antimicrobial activity

This study demonstrated the enhanced antimicrobial activity of co-cultured thermophilic microbes, *A. fumigatus* and *B. paramycooides*, and identified the metabolites induced during co-culture fermentation. The extract from single and co-culture fermentation contained secondary metabolites capable of inhibiting the pathogenic microorganisms tested. However, the highest antimicrobial activity was obtained from the co-culture against *E. coli*, *S. aureus*, and *C. albicans*, with mean clear zones of 20.33 ± 0.59 mm, 14.33 ± 0.59 mm, and 25.67 ± 0.59 mm, respectively (**Table 5**). These results indicated that the antimicrobial activity of the co-culture was stronger than that of the single-culture fermentation.

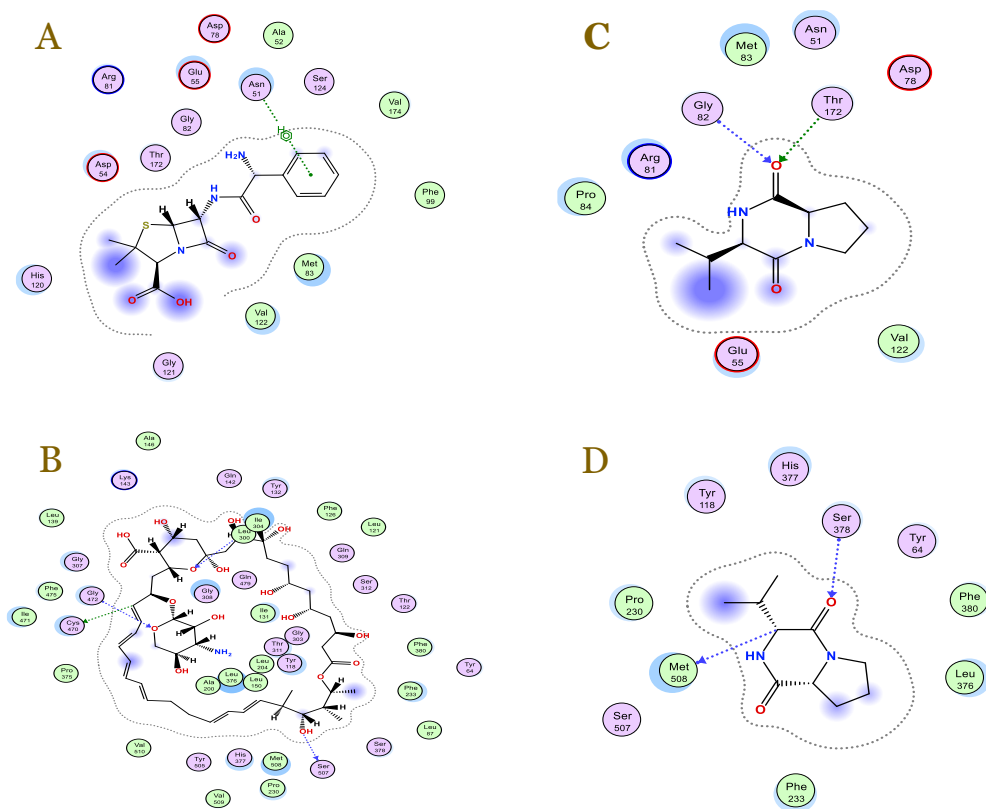


Figure 6. Residues involved in the interaction between ligand and enzyme receptor in 2D docking complexes. 2D Docking complex of the positive control (ampicillin) against topoisomerase IV enzyme (A) and the positive control (nystatin) against cytochrome monooxygenase CYP51 enzyme (B), as well as 3-(propan-2-yl)-octahydropyrrolo(1,2-a)pyrazine-1,4-dione against topoisomerase IV enzyme (C) and cytochrome monooxygenase CYP51 enzyme (D). Generated using the Maestro Ligand Interaction Diagram. Pink for hydrogen, green for hydrophobic.

Table 5. Antimicrobial activity of ethyl acetate extract from the fermentation of single *A. fumigatus*, *B. paramycooides*, and their co-culture using the disc diffusion method

Extracts	Average inhibition zone (mm), mean \pm SD		
	<i>C. albicans</i>	<i>S. aureus</i>	<i>E. coli</i>
<i>A. fumigatus</i>	23.33 \pm 0.59 ^b	12.33 \pm 0.59 ^d	13.67 \pm 0.59 ^c
<i>B. paramycooides</i>	22.67 \pm 0.59 ^b	13.33 \pm 0.59 ^c	11.33 \pm 0.59 ^d
Co-culture of <i>A. fumigatus</i> and <i>B. paramycooides</i>	25.67 \pm 0.59 ^a	14.33 \pm 0.59 ^b	20.33 \pm 0.59 ^b
Nystatin	25.00 \pm 0.59 ^a	-	-
Ampicillin	-	18.67 \pm 0.59 ^a	21.67 \pm 0.59 ^a

^{a-d} Values in the same column with different superscripts are significantly different at $p < 0.05$, as determined by Duncan's multiple range test

Discussion

Our data indicated that the samples from different fermentation conditions are separated and different from each other, indicating obvious differences in metabolite structures (**Figure 2**). This is consistent with the results of co-culture research between *Lactocaseibacillus casei* and *Lactiplantibacillus plantarum*, which showed differences in metabolite profiles in single culture and co-culture using a non-targeted metabolomics approach [13]. The fungus *A. fumigatus* could produce certain compounds due to the presence of *B. paramycooides*, and conversely, *B. paramycooides* could produce certain compounds due to the presence of the fungus. Most of the specific metabolic responses that occur in co-culture may be caused by bacterial responses to fungi [31].

Microbial co-culture fermentation has been widely explored as a strategy to enhance metabolite production by stimulating interactions between different microbial species. In present study, metabolomic profiling reveal that some metabolite-induced and other putatives in co-

culture group were increased in their production. The 2,6-bis(1,1-dimethylethyl)-4-methylphenol, tetradecane, and 2-(1,1-dimethylethyl) sulfonyl 2 methylpropane were produced in each single culture fermentation and increased in co-culture fermentation. The main volatile compound produced in co-culture was the phenolic compound 2,6-bis (1,1-dimethylethyl)-4-methylphenol. Phenolic compounds 2,6-bis(1,1-dimethylethyl)-4-methylphenol have been previously studied and showed antimicrobial activity against enterobacteria [32], antibacterial, antifungal, and antioxidant activity produced by fungi and bacteria [33]. Furthermore, another study reported that the compound provided promising potential antioxidant effects, especially in reducing free radicals 1,1-diphenyl-2-picryl-hydrazyl [34]. Another putative compound, tetradecane, was produced in each of the individual cultures of fungi and bacteria as well as in the co-culture. Tetradecane is also produced by the fungus *Penicillium pusillum* [35], the thermophilic bacterium *Streptomyces* sp. [36], and by plants as genotoxic volatile metabolites [37]. Tetradecane is used by plants to attract insects [38] and also acts as an antimicrobial agent [39]. Octadecanal and pentadecane are only produced by *A. fumigatus* fermentation and are enhanced in co-culture. Octadecanal is also a lipophilic phytochemical component found in the yellow and amber leaves of *Parrotia persica* [40] and a volatile compound in saliva, indicative of submandibular abscess due to bacterial activity [41]. Pentadecane is a volatile attractant produced by the fungus *Itajahya rosea* and used to attract *Drosophila* [42]. Volatile organic compounds can also be organic compounds containing sulfur [43]. In this study, there was also 2-(1,1-dimethylethyl)sulfonyl-2-methylpropane, which increased under co-culture fermentation conditions. The observed increase in secondary metabolites aligns with previous studies [44,45], suggesting that co-culture fermentation enhances metabolite production. Similar trends have been reported, where microbial interactions in co-cultures stimulate biosynthetic pathways, leading to higher yields [46,13]. These results further support the effectiveness of co-culture strategies in optimizing metabolite production.

Several reported studies have shown that the compounds produced by these local strains of thermophilic fungi and bacteria have bioactivity, including antimicrobial activity [47],[48],[49]. Pentadecanoic acid is a long-chain fatty acid with antimicrobial [50], antifungal, and antibacterial activity [51]. Pentadecanoic acid has been reported to have anti-biofilm properties against *C. albicans* and *Klebsiella pneumonia* [52]. Fatty acids and their derivatives also have been reported as good antimicrobial agents. *B. toyonensis* produced fatty acids that inhibited Gram-positive and negative bacteria and fungi [53]. The antibacterial activity of fatty acids and their derivatives is related to their membrane destabilizing and cell lysing activity on bacteria [54]. The present study also identified one of the fatty acid compounds in the form of pentadecanoic acid as a compound that was induced under co-culture conditions.

Fungi and bacteria engage in physical interactions during co-culture, triggering complex metabolic changes in both organisms and resulting in the production of diverse secondary metabolites. These changes are often driven by competition for space and nutrients, as well as the pressure exerted by the presence of competing microbes [55]. Such conditions can induce the production of new compounds, as observed in the co-culture of *Trichoderma harzianum* M10 and *Talaromyces pinophilus* F36CF [56]. Microbial co-cultures produce metabolites like signaling molecules, suppressive agents, and antimicrobials to enhance their competitiveness. For instance, *Ganoderma pfeiferi* has demonstrated antagonistic effects against bacteria and fungi, with its volatile compounds showing antimicrobial activity against *S. aureus*, *B. subtilis*, *E. coli*, and *C. albicans* [57]. Fungi, in general, are capable of producing various volatile organic compounds, including aldehydes, alcohols, acids, esters, ethers, ketones, thiols, terpenes, and their derivatives, which can act as antimicrobial agents [58].

In the present study, the top-five metabolites produced in the co-culture fermentation with the highest variable importance in projection values and the highest concentrations were methylbutylnitrisamine (m/z 116.10732), 2-(4-hydroxybenzyl)-4-(3-acetyl) quinoxalin-one (m/z 295.14145), mefenamic acid (m/z 241.99968), (aminomethyl) phosphonate (m/z 112.00661) and caprolactam (m/z 113.56815). The 2-(4-Hydroxybenzyl)-4-(3-acetyl) quinazolinone was also produced by *Aspergillus sydowii* SW9 in the previous study [59], and showed antimicrobial activity against human pathogenic bacteria *E. coli*, *S. aureus*, *S. epidermidis*, and *Streptococcus pneumoniae*, with minimum inhibitory concentration (MIC) values of 2.0 to 16 µg/mL [60]. The

compound 2-(4-hydroxybenzyl)-4-(3-acetyl) quinoxalin-one is a group of alkaloid compounds of the quinazoline type which has the potential as antimicrobial compounds [61]. To identify metabolites induced in co-culture fermentation, including known and potentially novel antimicrobial compounds, this present study was further analyzed using GNPS molecular networking.

Visualization of the molecular network with GNPS provided a schematic of the production of different metabolites under specific conditions [62]. Our data showed that co-culturing *A. fumigatus* and *B. paramycoides* led to the production of distinct compounds. Molecular networking effectively revealed metabolic profile alterations and facilitated the identification of bioactive compounds. In the present study, 3-alkyl indole was found only in the co-culture. There were five ionic features in the 3-alkyl indole cluster, including (m/z 370.259) or N1, m/z 352.249 (N2), m/z 336.254 (N3), m/z 354.264 (N4) and m/z 372.275 (N5). This indicated a close structural relationship between N1-N5. Features that are in the same cluster indicate that they have a very close structural relationship [63]. Tryptamine was detected only in the single culture of *B. paramycoides* and co-culture, but not in the single culture of *A. fumigatus*. In *B. paramycoides* fermentation, tryptamine was identified with molecular weights m/z 413.353 and m/z 399.337, while in co-culture fermentation, it appeared as m/z 441.385 (N6). Tryptamine, an indole-derived alkaloid from the essential amino acid tryptophan, has been previously reported in co-cultures of *Streptomyces* and *B. mycoides*, where it induced tryptamine derivatives (N-acetyltryptamine, N-propanoyltryptamine, and bacillamide) with algicidal activity [64].

Other compounds induced in co-culture fermentation, as identified through molecular networking, were pyrazines, including m/z 194.975 (N7), m/z 195.088 (N8), and m/z 244.264 (N9). LC-MS/MS analysis detected m/z 196.1213, corresponding to the molecular formula $C_{10}H_{16}N_2O_2$, identified as 3-(propane-2-yl)-octahydropyrrolo(1,2-a)pyrazine-1,4-dione. This suggested that N7 and N8 are derivatives of this compound, differing by the release of two and one hydrogen molecules, respectively, while N9 is likely another pyrazine derivative. Pyrazines, known for their antifungal properties, have been reported in *Paenibacillus*, demonstrating strong inhibitory activity against *Burkholderia* and various plant and human pathogens [12,63].

Molecular networking with GNPS demonstrated that 13 molecular clusters were exclusively induced in the co-culture (numbered N1-N13) (**Figure 5**). It is suggested that metabolites N1-N5 are derivatives of indole derivatives compounds, while N6 is believed to be a derivative of tryptamine compounds. It was proposed that N7-N9 were derivatives of the compound 3-(propane-2-yl)-octahydropyrrolo(1,2-a)pyrazine-1,4-dione, while N10-N13 were assumed to be derivatives of the lipid compound 3-phosphoethanolamine. A metabolomic analysis of the diversity of compounds produced in co-culture fermentation will facilitate the discovery of induced compounds and provide a valuable opportunity for the identification of new compounds in a more time-efficient manner [20]. Previous study has indicated that mass spectrometry and molecular network results obtained from GNPS have revealed that co-cultures of *Aspergillus terreus* and *A. unguis* tend to maintain dominance through the synthesis of secondary metabolites and the production of chlorinated compounds by *A. unguis* [65]. This study highlights 3-(propane-2-yl)-octahydropyrrolo (1,2-a)pyrazine-1,4-dione as a key alkaloid compound predominantly produced under co-culture conditions. Alongside alkyl indole derivatives and tryptamine, this novel pyrazine derivative was identified as a major metabolite. Metabolomic analysis further demonstrated that 3-(propane-2-yl)-octahydropyrrolo(1,2-a)pyrazine-1,4-dione exhibited significant antimicrobial activity, emphasizing its potential as a promising bioactive compound for antimicrobial applications.

The compound 3-(propane-2-yl)-octahydropyrrolo(1,2-a)pyrazine-1,4-dione was subjected to molecular docking studies using MOE 2020.0102 to investigate its potential binding modes with specific enzyme targets. The conformation with the lowest binding energy was selected as the most favorable interaction between the ligand and receptor. Topoisomerase IV was chosen as the antibacterial target due to its essential role in maintaining DNA topology during transcription and replication, making it a well-established target for antibacterial drugs [30,28]. Docking analysis revealed that the compound bound effectively to the DNA topoisomerase IV receptor (**Figure 6C**) with a binding energy of -5.34 kcal/mol. The binding site exhibited a similar binding conformation to that of the co-crystallized OR9 ligand, which exhibited a minimum binding

energy of -9.04 kcal/mol. Notably, the 1-O group of the compound formed hydrogen bonds with Thr 172 and Gly 82, further supporting its observed antimicrobial activity.

For antifungal activity, cytochrome monooxygenase was selected as the target enzyme due to its critical role in the ergosterol biosynthesis pathway. Ergosterol is an essential component of fungal cell membranes, and disruptions in its synthesis can lead to loss of membrane integrity and fungal cell death, making cytochrome monooxygenase a promising target for antifungal drug development [66]. Molecular docking results demonstrated that 3-(propane-2-yl)-octahydropyrrolo(1,2-a)pyrazine-1,4-dione exhibited strong binding to cytochrome monooxygenase, supported by hydrophobic interactions and hydrogen bonds with residues Met 508 and Ser 378 (**Figure 6D**). These findings underscore the potential of this compound as a dual-action antimicrobial agent, effectively targeting both bacterial and fungal pathogens.

Based on the antimicrobial test, ethyl acetate extract from co-culture fermentation has the potential to inhibit gram-negative, and gram-positive bacteria and also pathogenic fungi. There is a difference in the diameter of the inhibition zone for all three test microbes, indicating that there were differences in sensitivity to the test microbes. The results of the inhibition zone of the co-culture fermentation extracts are significantly different from each single culture, this can also be seen from the results of the Duncan test, indicated by the superscript letters, which are not the same. Clear results of the antimicrobial test were observed for all extracts at a concentration of 120 ppm, indicating that the co-culture fermented extracts had strong antimicrobial properties. The increase in antimicrobial activity is largely determined by the bioactive compounds produced by the microbes during co-culture. The results of previous research on the co-culture of *A. fumigatus* showed the existence of new induced compounds with various bioactivities. As with the co-culture of *A. fumigatus* from mine drainage water with *Sphingomonas*, a new diketopiperazine antibiotic in the form of Gionitrin A was successfully induced. Gionitrin A showed significant antibiotic activity against a range of microbes, including methicillin-resistant *Staphylococcus aureus* [67].

While our findings highlight the potential of co-culture fermentation in enhancing antimicrobial compound discovery, this study primarily relies on in silico analysis (molecular docking) without extensive experimental validation of compound-target interactions. Although the antimicrobial activity of the extracts has been demonstrated, the specific contributions of individual bioactive metabolites remain unclear, requiring further isolation and characterization. Additionally, variations in fermentation conditions may influence metabolite production, necessitating further optimization and standardization to ensure reproducibility. To address these limitations, future research should focus on isolating and characterizing individual bioactive compounds, conducting in vitro and in vivo validation of their antimicrobial mechanisms, and optimizing fermentation conditions to enhance metabolite yield and consistency.

Conclusion

Metabolomic profiling using GC-MS and LC-HRMS revealed an increase in antimicrobial metabolites in co-culture fermentation extracts of *A. fumigatus* and *B. paramycoides*. The identified compounds include pentadecanoic acid, cyclopropane pentanoic acid, 3-piperidinol, 2-(4-hydroxybenzyl)-4-(3-acetyl)quinazolinone, five novel 3-alkyl indoles (N1-N5), and two novel pyrazine derivatives (N7 and N8), putatively derived from 3-(propan-2-yl)-octahydropyrrolo(1,2-a)pyrazine-1,4-dione. Notably, compounds N7 and N8 were exclusively produced through the co-culture of *A. fumigatus* and *B. paramycoides*. Molecular docking studies with topoisomerase IV and cytochrome monooxygenase revealed that 3-(propan-2-yl)-octahydropyrrolo(1,2-a)pyrazine-1,4-dione was the most promising compound, as indicated by its lower binding energy values. Additionally, the significant antimicrobial activity observed in the co-culture extract highlighted the potential of co-culture fermentation technique. This method not only enhanced the antimicrobial properties of metabolites but also induced the production of novel bioactive compounds. Future studies are required to isolate target compounds, such as N7 and N8, in pure form to confirm their structural identity and biological activity. Moreover, determining the minimum inhibitory concentration values of these compounds against specific pathogens will provide deeper insights into their potency as antimicrobial agents.

Ethics approval

Ethical approval is not required.

Acknowledgments

The authors would like to thank the entire committee of the 2024 Annual Scientific Meeting (PIT) of the Indonesian Society for Clinical Microbiologists and their respective affiliated universities.

Competing interests

All authors declare that they have no competing interests.

Funding

No external funding is received.

Underlying data

The underlying data can be requested from the corresponding author.

Declaration of artificial intelligence use

This study used artificial intelligence (AI) tools for manuscript writing support. Specifically, AI-based language model, ChatGPT, was employed for language refinement, including improving grammar, sentence structure, and readability of the manuscript. We confirm that all AI-assisted processes were critically reviewed by the authors to ensure the integrity and reliability of the results. The final decisions and interpretations presented in this article were solely made by the authors.

How to cite

Octarya Z, Nugroho TT, Nurulita Y, *et al.* Enhanced antimicrobial activity and metabolomic profiling of the *Aspergillus fumigatus* LBKURCC269 co-cultured with *Bacillus paramycooides* LBKURCC218. Narra J 2025; 5 (2): e1647 - <http://doi.org/10.52225/narra.v5i2.1647>.

References

1. Webale MK, Guyah B, Wanjala C, *et al.* Phenotypic and genotypic antibiotic resistant diarrheagenic *Escherichia coli* pathotypes isolated from children with diarrhea in Nairobi City, Kenya. Ethiop J Health Sci 2020;30(6):881-890.
2. Tummanapalli SS, Willcox MD. Antimicrobial resistance of ocular microbes and the role of antimicrobial peptides. Clin Exp Optom 2021;104(3):295-307.
3. Prastiyanto ME, Darmawati S, Daryono BS, *et al.* Examining the prevalence and antimicrobial resistance profiles of multidrug-resistant bacterial isolates in wound infections from Indonesian patients. Narra J 2024;4(2):1-13.
4. Octarya Z, Novianty R, Suraya N, *et al.* Antimicrobial activity and gc-ms analysis of bioactive constituents of *Aspergillus fumigatus* 269 isolated from sungai pinang hot spring, Riau, Indonesia. Biodiversitas 2021;22(4):1839-1845.
5. Octarya Z, Nugroho TT, Yuana N, *et al.* Molecular identification, gc-ms analysis of bioactive compounds and antimicrobial activity of thermophilic bacteria derived from West Sumatra hot-spring Indonesia. Hayati J Biosci 2022;29(4):550-561.
6. Mahajan GB, Balachandran L. Sources of antibiotics: Hot springs. Biochem Pharmacol 2017;134(11):35-41.
7. Ojha P, Prasad N, Shreenath K, *et al.* Isolation of a broad spectrum antimicrobial producing thermophilic *Bacillus* and characterization of its antimicrobial protein. Arch Microbiol 2021;203(5):2059-2073.
8. Aissaoui N, Mahjoubi M, Nas F, *et al.* Antibacterial potential of 2, 4-di-tert-butylphenol and calixarene-based prodrugs from thermophilic *Bacillus licheniformis* isolated in algerian hot spring from thermophilic *Bacillus licheniformis* isolated in algerian hot spring. Geomicrobiol J 2018;0(0):1-10.
9. Bertrand S, Bohni N, Schnee S, *et al.* Metabolite induction via microorganism co-culture: A potential way to enhance chemical diversity for drug discovery. Biotechnol Adv 2014;32(6):1180-1204.
10. Selegato DM, Castro-Gamboa I. Enhancing chemical and biological diversity by co-cultivation. Front Microbiol 2023;14(2):1-24.

11. Tan ZQ, Leow HY, Lee DCW, *et al.* Co-culture systems for the production of secondary metabolites: Current and future prospects. *Open Biotechnol J* 2019;13(1):18-26.
12. Tyc O, de Jager VCL, van den Berg M, *et al.* Exploring bacterial interspecific interactions for discovery of novel antimicrobial compounds. *Microb Biotechnol* 2017;10(4):910-925.
13. Guo S, Li B, Wang D, *et al.* Metabolomic analysis of cooperative adaptation between co-cultured *Lactocaseibacillus casei* zhang and *Lactiplantibacillus plantarum* p8. *Lwt* 2022;170,114105.
14. Ueda K, Beppu T. Antibiotics in microbial coculture. *J Antibiot* 2017;70(4):361-365.
15. König CC, Scherlach K, Schroeckh V, *et al.* Bacterium induces cryptic meroterpenoid pathway in the pathogenic fungus *Aspergillus fumigatus*. *ChemBioChem* 2013;14(8):938-942.
16. Wakefield J, Hassan HM, Jaspars M, *et al.* Dual induction of new microbial secondary metabolites by fungal bacterial co-cultivation. *Front Microbiol* 2017;8(7):1-10.
17. Wu Qiong, Dou Kai, Tang Jun, *et al.* Co-culture of *Bacillus amyloliquefaciens* ACCC11060 and *Trichoderma asperellum* GDFS1009 enhanced pathogen-inhibition and amino acid yield. *Microb Cell Factories* 2018;17(17):155.
18. Yao L, Zhu LP, Xu XY, *et al.* Discovery of novel xylosides in co-culture of basidiomycetes *Trametes versicolor* and *Ganoderma applanatum* by integrated metabolomics and bioinformatics. *Sci Rep* 2016;6(81-13).
19. Morales N, Ferreira L, Oliveira P De, *et al.* Elicitation of *Streptomyces lunalinharesii* secondary metabolism through co-cultivation with *Rhizoctonia solani*. *Microbiol Res* 2021;251(1):126836.
20. Arora D, Gupta P, Jaglan S, *et al.* Expanding the chemical diversity through microorganisms co-culture: Current status and outlook. *Biotechnol Adv* 2020;40(1):107521.
21. Octarya, Z, Nugroho TT, Nurulita Y, Suraya NS. Production of antifungal compounds from *Bacillus paramycooides* lbkurcc218 and *Aspergillus fumigatus* lbkurcc269 co-cultivation. *Mater Today Proc* 2023;87(2):120-125.
22. Zhang Q, Wang SQ, Tang HY, *et al.* Potential allelopathic indole diketopiperazines produced by the plant endophytic *Aspergillus fumigatus* using the one strain-many compounds method. *J Agric Food Chem* 2013;61(47):11447-11452.
23. Rateb ME, Hallyburton I, Houssen WE, *et al.* Induction of diverse secondary metabolites in *Aspergillus fumigatus* by microbial co-culture. *RSC Adv* 2013;3(34):14444-14450.
24. Abdelkareem S, Hassan A, Elhaj S, *et al.* Optimization of Antibacterial Compounds Production by *Aspergillus fumigatus* Isolated from Sudanese Indigenous Soil. *Int Biomed Biol J* 2017;3(4):203-208.
25. Chaudhary R, Tripathy A. Isolation and identification of bioactive compounds from *Irpex Lacteus* wild fleshy fungi. *J Pharm Sci Res* 2015;7(7):424-434.
26. Ernst M, Kang K Bin, Nothias L felix, *et al.* Molnetenhancer : Enhanced molecular networks by integrating metabolome mining and annotation tools. *Metabolites* 2019;9(144).
27. Aron AT, Gentry EC, McPhail KL, *et al.* Reproducible molecular networking of untargeted mass spectrometry data using GNPS. *Nat Protoc* 2020;15(6):1954-1991.
28. Duraipandiyani V, Al-Dhabi NA, balachandran c, *et al.* Novel 1,5,7-trihydroxy-3-hydroxy methyl anthraquinone isolated from terrestrial streptomyces sp. (eri-26) with antimicrobial and molecular docking studies. *Appl Biochem Biotechnol* 2014;174(5):1784-1794.
29. Umar AH, Ratnadewi D, Rafi M, *et al.* Untargeted metabolomics analysis using ftir and uhplc-q-orbitrap hrms of two *Curculigo* species and evaluation of their antioxidant and α -glucosidase inhibitory activities. *Metabolites* 2021;11(1):1-17.
30. Wang W, Chen R, Luo Z, *et al.* Antimicrobial activity and molecular docking studies of a novel anthraquinone from a marine-derived fungus *Aspergillus versicolor*. *Nat Prod Res* 2018;32(5):558-563.
31. Nicault M, Zaiter A, Dumarcay S, *et al.* Elicitation of antimicrobial active compounds by streptomyces-fungus co-cultures. *Microorganisms* 2021;9(1):1-13.
32. Mitani T, Ota K, Inaba N, *et al.* Antimicrobial activity of the phenolic compounds of *Prunus mume* against enterobacteria. *Biol Pharm Bull* 2018;41(2):208-212.
33. Fuqiang Z, Ping W, Rima D, *et al.* Natural sources and bioactivities of 2,4-di-tert-butylphenol and its analogs. *Toxins* 2020;12(35):1-26.
34. Ibtissem B, Imen M, Souad S. Dosage of 2,6-Bis (1,1-Dimethylethyl)-4-Methylphenol (BHT) in the plant extract *Mesembryanthemum crystallinum*. *J Biomed Biotechnol* 2010;2010:1-5.
35. Ghanbari MAT, Mohammadkhani HS, Babaeizad V, *et al.* Identification of some secondary metabolites produced by four *Penicillium* species. *Mycol Iran* 2014;1(10):107-113.
36. Al-Dhabi NA, Duraipandiyani V, Arasu MV, *et al.* Antifungal metabolites from sponge associated marine streptomyces sp. Strain (ERIMA-01). *J Pure Appl Microbiol* 2014;8(1):115-128.

37. Kim JK, Shin HS, Lee JH, *et al.* Genotoxic effects of volatile organic compounds in a chemical factory as evaluated by the Tradescantia micronucleus assay and by chemical analysis. *Mutat Res - Genet Toxicol Environ Mutagen* 2003;541(1-2):55-61.
38. Wang X, Wang S, Yi J, *et al.* Three host plant volatiles, hexanal, lauric acid, and tetradecane, are detected by an antenna-biased expressed odorant receptor 27 in the dark black chafer holotrichia parallela. *J Agric Food Chem* 2020;68(28):7316-7323.
39. Nahid Rahbar. Antimicrobial activity and constituents of the hexane extracts from leaf and stem of origanum vulgare L. Ssp. Viride (boiss.) Hayek. Growing wild in Northwest Iran. *J Med Plants Res* 2012;6(13):2681-2685.
40. Djapic N. Parrotia persica yellow and amber leaves' lipophilic phytochemicals obtained by supercritical carbon dioxide extraction. *Molecules* 2022;27(16).
41. Monedeiro F, Milanowski M, Ratiu IA, *et al.* VOC profiles of saliva in assessment of halitosis and submandibular abscesses using HS-SPME-GC/MS technique. *Molecules* 2019;24(16).
42. Borde M, Kshirsagar Y, Jadhav R, *et al.* A rare stinkhorn fungus itajahya rosea attract drosophila by producing chemical attractants. *Mycobiology* 2021;49(3):223-234.
43. Caulier S, Nannan C, Gillis A, *et al.* Overview of the antimicrobial compounds produced by members of the *Bacillus subtilis* group. *Front Microbiol* 2019;10(2):1-19.
44. Wu Q, Ni M, Dou K, *et al.* Co-culture of *Bacillus amyloliquefaciens* ACCC11060 and *Trichoderma asperellum* GDFS1009 enhanced pathogen-inhibition and amino acid yield. *Microb Cell Factories* 2018;17(1):1-12.
45. Li J, Zhang L, Yao G, *et al.* Synergistic effect of co-culture rhizosphere Streptomyces: A promising strategy to enhance antimicrobial activity and plant growth-promoting function. *Front Microbiol* 2022;13(8):1-18.
46. Li W, Fu Y, Jiang Y, *et al.* Synergistic biocontrol and growth promotion in strawberries by co-cultured trichoderma harzianum tw21990 and burkholderia vietnamiensis b418. *J Fungi* 2024;10(8):551.
47. Panda AK, Bisht SS, Rana M, *et al.* Biotechnological potential of thermophilic actinobacteria associated with hot springs. Elsevier B.V.; 2018.
48. Prasad GS. Fungi in extreme environments: Ecological role and biotechnological significance. *Fungi extreme environ ecol role biotechnol significance* 2019:269-289.
49. Orfali R, Perveen S. New bioactive metabolites from the thermophilic fungus penicillium sp. Isolated from ghamiqa hot spring in saudi arabia. *J Chem* 2019;2019.
50. Chandrasekaran M, Kannathasan K, Venkatesalu V. Antimicrobial activity of fatty acid methyl esters of some members of chenopodiaceae. *Z Naturforschung -Sect C J Biosci* 2008;63(5-6):331-336.
51. Agoramoorthy G, Chandrasekaran M, Venkatesalu V, *et al.* Antibacterial and antifungal activities of fatty acid methyl ester of the blind-your eye mangrove from India. *Braz J Microbiol* 2007:739-742.
52. Galdiero E, Ricciardelli A, D'Angelo C, *et al.* Pentadecanoic acid against candida albicans-klebsiella pneumoniae biofilm: towards the development of an anti-biofilm coating to prevent polymicrobial infections. *Res Microbiol* 2021;172(7-8):103880.
53. Gad AM, Beltagy EA, Abdul-Raouf UM, *et al.* Screening of marine fatty acids producing bacteria with antimicrobial capabilities. *Chem Adv Mater* 2016;1(2):41-54.
54. Yoon BK, Jackman JA, Valle-González ER, *et al.* Antibacterial free fatty acids and monoglycerides: biological activities, experimental testing, and therapeutic applications. *Int J Mol Sci.* 2018;19(4):1114.
55. Yu M, Li Y, Banakar SP, *et al.* New metabolites from the co-culture of marine-derived actinomycete streptomyces rochei mb037 and fungus rhinocladiella similis35. *Front Microbiol* 2019;10(5):1-11.
56. Vinale F, Nicoletti R, Borrelli F, *et al.* Co-culture of plant beneficial microbes as source of bioactive metabolites. *Sci Rep* 2017;7(1):1-12.
57. Mothana RAA, Jansen R, Jülich WD, *et al.* Ganomycins a and b, new antimicrobial farnesyl hydroquinones from the basidiomycete ganoderma pfeifferi. *J Nat Prod* 2000;63(3):416-418.
58. Geesink P, Tyc O, Küsel K, *et al.* Growth promotion and inhibition induced by interactions of groundwater bacteria. *FEMS Microbiol Ecol* 2018;94(11):1-8.
59. Orfali R, Aboseada MA, Abdel-wahab NM, *et al.* Recent updates on the bioactive compounds of the marine-derived genus *Aspergillus*. *RSC Adv.* 2021;11(28):17116-17150.
60. Liu YJ, Zhang JL, Li C, *et al.* Antimicrobial secondary metabolites from the seawater-derived fungus *Aspergillus sydowii* sw9. *Molecules* 2019;24(24):4-11.
61. Willems T, De Mol ML, De Bruycker A, *et al.* Alkaloids from marine fungi: Promising antimicrobials. *Antibiotics* 2020;9(6):1-27.

62. Vitale GA, Sciarretta M, Cassiano C, *et al.* Molecular network and culture media variation reveal a complex metabolic profile in *Pantoea* cf. *Eucrina* d2 associated with an acidified marine sponge. *Int J Mol Sci* 2020;21(17):1-18.
63. Sun Y, Liu WC, Shi X, *et al.* Inducing secondary metabolite production of *Aspergillus sydowii* through microbial co-culture with *Bacillus subtilis*. *Microb Cell Factories* 2021;20(1):1-16.
64. Yu L, Hu Z, Ma Z. Production of bioactive tryptamine derivatives by co-culture of marine *Streptomyces* with *Bacillus mycoides*. *Nat Prod Res* 2015;29(22):2087-2091.
65. Wang Y, Glukhov E, He Y, *et al.* Secondary metabolite variation and bioactivities of two marine *Aspergillus* strains in static co-culture investigated by molecular network analysis and multiple database mining based on LC-PDA-MS/MS. *Antibiotics* 2022;11(4).
66. Abdella B, Abdella M, ElSharif HA, *et al.* Identification of potent anti-candida metabolites produced by the soft coral associated streptomyces sp. Hc14 using chemoinformatics. *Sci Rep* 2023;13(1):1-10.
67. Park HB, Kwon HC, Lee CH, *et al.* Glionitrin A, an antibiotic - antitumor metabolite derived from competitive interaction between abandoned mine microbes. *J Nat Prod* 2009;72(2):248-252.